

Effects of window opening style on inside environment of solar greenhouse based on CFD simulation

Yachen Sun^{1†}, Encai Bao^{2†}, Chenmeng Zhu³, Lulu Yan^{1,4}, Yanfei Cao¹, Xuanhe Zhang¹,
Jianming Li¹, Haiwei Jing^{5*}, Zhirong Zou^{1*}

(1. Key Laboratory of Protected Horticultural Engineering in Northwest, Ministry of Agriculture, Department of Horticulture, Northwest A&F University, Yangling 712100, Shaanxi, China; 2. Institute of Agricultural Facilities and Equipment, Jiangsu Academy of Agricultural Science, Key Laboratory of Protected Agriculture Engineering in the Middle and Lower Reaches of Yangtze River, Ministry of Agriculture and Rural Affairs, Nanjing 210014, China; 3. College of Management, City University of Hong Kong, Tat Chee Avenue, Kowloon 999077, Hong Kong, China; 4. Department of Horticulture, Xinyang Agriculture and Forestry University, Xinyang 464000, Henan, China; 5. Department of Water Resources and Architectural Engineering, Northwest A&F University, Yangling 712100, Shaanxi, China)

Abstract: Solar greenhouse is extensively used in horticultural production in China. Natural ventilation is one of the key technological means to adjust the inside environment of greenhouse, while the effects of window opening styles on the inside environment are still not well understood. In the present study, the temperature and air flow field of five operation styles, namely back roof central opening style (G1), back roof evenly spaced opening style (G2), top roof full opening style (G3), style of G1+G3, and style of G2+G3 were simulated using the CFD method. The results indicated that: (1) the simulated and measured results exhibited favorable agreement, with relative errors within 5%; (2) In the case of the windows opening area was the same and only single ventilation style was applied, back roof full opening style exhibited the best cooling effect. The inside average temperature of the greenhouse with G1 style decreased by 0.5 °C and 1.6 °C respectively compared with those of greenhouses with G2 and G3. (3) The cooling effect of the style of G2+G3 was more favorable than that of the style of G1+G3. The style of G2+G3 exhibited better cooling effect than the single ventilation styles, with the lowest temperature (27.5 °C) and temperature uniformity coefficient (0.36).

Keywords: CFD modeling, window opening styles, cooling effects, solar greenhouse

DOI: 10.25165/j.ijabe.20201306.5734

Citation: Sun Y C, Bao E C, Zhu C M, Yan L L, Cao Y F, Zhang X H, et al. Effects of window opening style on inside environment of solar greenhouse based on CFD simulation. *Int J Agric & Biol Eng*, 2020; 13(6): 53–59.

1 Introduction

Solar greenhouse is extensively used in China for its favorable heat preservation and energy saving characteristics. According to the data from the former department of agricultural mechanization management of ministry of agriculture of China, the total area of solar greenhouse has reached 6.6×10^5 hm² to the end of 2016, accounting 31.8% of the agricultural facilities. Utilization of greenhouse ensures the vegetable supply for Northern China in winter, and it also provides important approach to adjust the agricultural structure^[1].

During the horticultural production in solar greenhouse, ventilation is one of the key technological means to adjust the inside environment^[2,3]. Natural ventilation, that is, the air motion caused by wind and thermal pressure through window, can dissipate extra heat and bring fresh air and CO₂ into greenhouse. It also can dissipate extra vapor, thus decreasing the humidity and providing favorable environmental conditions for the plants in greenhouses^[4].

Numerous factors had been confirmed which affecting the efficiency of natural ventilation. For instances, Mistriotis et al.^[5] indicated that the factors influence the greenhouse ventilation including the wind direction and speed, the outside irradiance, the temperature difference between the inside and outside of greenhouse, the overall structure of greenhouse, as well as the size, shape and position of windows. Wei et al.^[6] found that the single span greenhouse with removable back walls exhibits better ventilation and cooling efficiency than the traditional greenhouses. Xie et al.^[7] indicated that the temperature and moisture of northern greenhouse using roof ventilation decrease with the increasing outside natural wind speed. In addition, to cover the shortages of theoretical analyzing method, computational simulations were also extensively used. In the existing simulating methods, the computational fluid dynamics (CFD) provides various numerical solution, which are helpful in the investigations of fluid flow, heat transmission and chemical reaction^[8], especially in the research of ventilation and heat transmission^[9-11], and thus reduces the workload of experiments. For examples, Bournet and Boulard^[12]

Received date: 2020-02-15 **Accepted date:** 2020-08-17

Biographies: **Yachen Sun**, PhD candidate, research interests: facility horticulture, Email: sunyachen1993@163.com; **Encai Bao**, PhD, Assistant Research Fellow, research interests: facility horticulture engineering, Email: baoencai1990@163.com; **Chenmeng Zhu**, Master candidate, research interests: organizational management, Email: cmzhu4-c@my.cityu.edu.hk; **Lulu Yan**, Master candidate, research interests: facility horticulture engineering, Email: luluyande@163.com; **Yanfei Cao**, PhD, research interests: greenhouse structure optimization, Email: caoyanfei@nwsuaf.edu.cn; **Xuanhe Zhang**, Master candidate, research interests: facility horticulture engineering, Email: 798093267@qq.com; **Jianming Li**, PhD, Professor, research interests: facility horticulture engineering and physiological cultivation, Email: lijianming66@163.com.

†These authors contribute equally to this research.

***Corresponding authors:** **Haiwei Jing**, PhD, Professor, research interests: natural ventilation theory and simulation. Tel: +86-18092867919, Email: 26144387@qq.com; **Zhirong Zou**, PhD, Professor, research interests: facility horticulture. Tel: +86-13991124991, Email: zouzhirong2005@163.com.

explored the mechanism of using CFD as a simulating approach and the availability of using it in the simulation of airflow environment. Baxevanou et al.^[13] used CFD for the thermal environment modeling of the mechanically ventilated glass greenhouse. In recent years, CFD had also been widely utilized in the studies of solar greenhouse. For instances, Song^[14] simulated the temperature distribution of a solar greenhouse. And it is showed that the simulated values were almost consistent with the detected values, which suggested that the CFD is available in the simulation of the inside environment of greenhouse. Chang^[15] used CFD for the simulation of the thermal and humidity in the greenhouse with traditional loam wall. Fang et al.^[16] set up the CFD model of the solar greenhouse using Fluent software, and solved the three-dimensional steady state of the distribution of the airflow in a solar greenhouse. Besides, the availability of CFD in the simulation of the inside environment of solar greenhouse with various wall materials, size, and constructions were also confirmed by numerous studies^[17-20]. In addition, the effects of different window opening style on the inside environment of solar greenhouse were also investigated. Using CFD simulation, investigators studied the ventilation efficiency, temperature and flow field conditions of the full open-roof glass greenhouse^[21]. He et al.^[22] studied the effects of different wind regime and vent configuration on the environment in tunnel greenhouses, indicating that the vent configuration dramatically affects the microclimate. The roof plus side opening provides the highest ventilation efficiency, and the thermal natural ventilation play a dominant role when the outside temperature is high and the wind speed is relative slow. Hence, the roof ventilation window plays important roles in the thermal ventilation. However, for the solar greenhouses, the dust and water retention are of frequent occurrence around the roof vents because of the impeded drainage, which will cause decreases in the luminousness and life span of greenhouse film. Furthermore, the dust retention will alter the width of partial vents, which will significantly affect the ventilation efficiency. Hence, relative to the traditional roof ventilation, the back slope ventilation might exhibit better cooling efficiency^[23,24], because it has more height difference between inlet and outlet of wind, and the characteristics of reducing the thermal storage of back roof.

The airflow pattern and distribution of temperature and moisture are quite different among greenhouses with different window opening styles^[25], while the homogeneity of inside microenvironment is quite important to the growth and development of crops in greenhouse. However, the relationship between back roof ventilation and greenhouse microenvironment is still not well understood, which obstructs the application of this ventilation form. In the present study, the temperatures at different positions inside greenhouses with top roof and 2 types of back roof ventilation were comparatively studied. Based on these, the CFD simulation was adopted to study of effect of different window opening styles on environmental indicators including temperature and air flow of the greenhouses.

2 Materials and methods

2.1 Investigated greenhouses

The investigated greenhouses located in the Northwest A&F University, Yangling District, Shaanxi, China (34°16'N, 108°06'E). The structure of the greenhouse was shown in Figure 1, which had a north-south span of 8 m, a length of 16 m, and a height of 3.6 m. The back wall with a height of 2.2 m was constructed with 780 mm

brick inner wall and 100 mm polystyrene outer board. The front roof was made of PO film with a thickness of 0.10 mm. A vent window of 0.8 m in width and 16 m in length was set on the front roof at the height of 0.65 m above the ground.

In order to investigate the effect of different vent style on inside environment of greenhouse, three greenhouses with the same vent area but different upper ventilation styles were designed. The greenhouse 1 (G1) was back roof central opening style, which is applied by using an 8.0 m×1.2 m window set on the back roof using the ridgeline as one edge (Figure 2a). The window was controlled by an electric window drive system, and the motor used was the 0.37 kW WJNA40-2.6 special reduction motor for greenhouse (HUANONG-BESKY Co., Ltd., Beijing, China). For greenhouse 2 (G2) was back roof evenly spaced opening style, which is applied by using eight windows with a size of 1.0 m×1.2 m and spacing of 2 m evenly set on the back roof, the ridgeline was also used as one edge for each window (Figure 2b). For greenhouse 3 (G3) was top roof full opening style, which is applied by using 16.0 m×0.6 m window was set on the top roof. All of the vent windows were covered with 52-mesh insect proof net. During the experiments, all of the windows for every greenhouse were full opened.

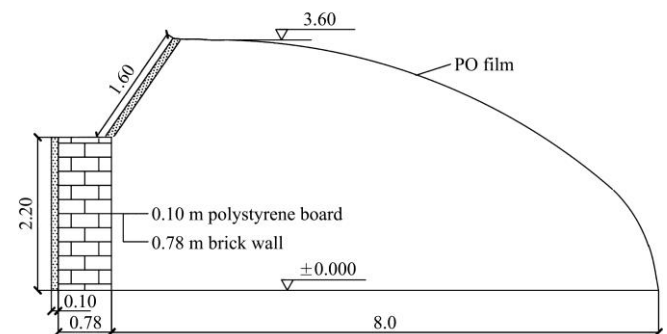
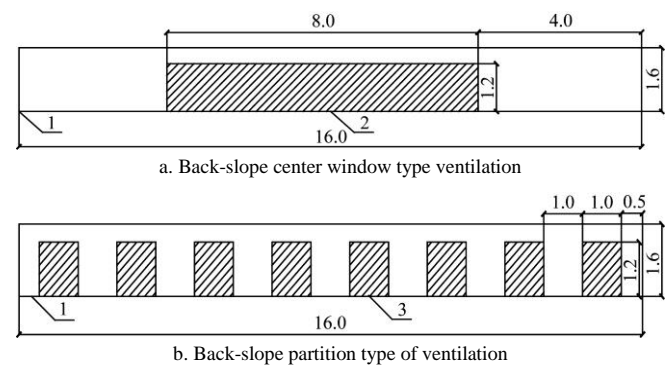


Figure 1 Structure of the investigated greenhouses (Unit: m)



1. Ridgeline of the greenhouses 2, 3. Windows on the backroof

Figure 2 Distribution of the windows on the back roof (Unit: m)

2.2 Data collection

The experiments were conducted in May 12th, 2019. Three typical cross sections were chosen from east to west in each greenhouse, and they were labeled as A, B and C (Figure 3a). Nine measurement points were set on each cross section and were named as A1-A9, B1-B9 and C1-C9, respectively. The layout of the 9 points was given in Figure 3b. The temperature was then determined and recorded using T type thermocouples (Herowire and cable Co., Ltd., Shanghai, China). The measurement range was -200 °C to 350 °C, with the accuracy of ±0.2 °C) and an Agilent data collector (Agilent Co., Ltd., USA). The time intervals of automatically record were 10 min. The outside air temperature and moisture, solar radiation and wind speed were determined

using a HOBO U30 portable automatic meteorological station, which has a temperature measurement range of $-40\text{ }^{\circ}\text{C}$ to $75\text{ }^{\circ}\text{C}$, with the accuracy of $\pm 0.7\text{ }^{\circ}\text{C}$; a moisture measurement range of 0-100%, with the accuracy of 3%; and a solar radiation (400-700 nm) measurement range of 0-1280 W/m^2 , with the accuracy of $\pm 10\text{ W}/\text{m}^2$ and the resolution of $1.25\text{ W}/\text{m}^2$. The automatic meteorological station was set up at the height of 1.5 m above the ground in an open area at the west of the greenhouse with a distance of 10m, and the mentioned data were collected every 1 min. The indoor and outside environmental parameters collected at 15:30 were used for the following model verification. At that time, the outside wind speed was 1.51 m/s, the solar radiation was $561.9\text{ W}/\text{m}^2$, and the temperature of the greenhouse entrance was $27.3\text{ }^{\circ}\text{C}$, respectively.

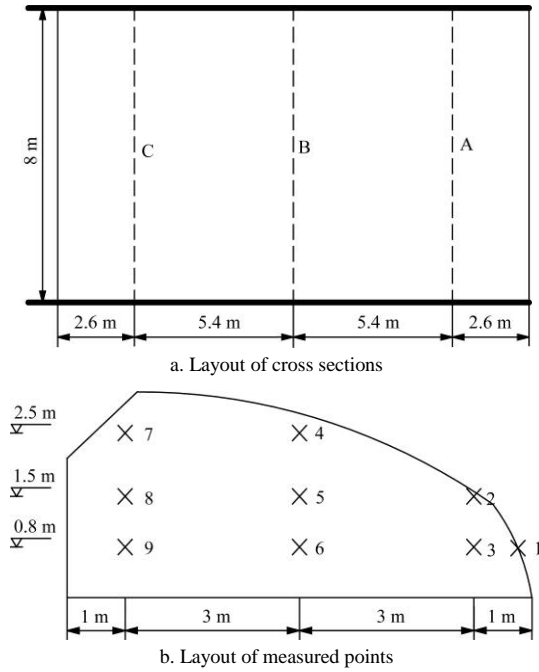


Figure 3 Layout of the indoor air temperature measurement points

The temperature uniformity coefficient is defined to evaluate the uniformity of indoor temperature,

$$\zeta = \frac{\sum_{i=1}^n (T_i - \bar{T})^2}{n} \quad (1)$$

where, ζ is the temperature uniformity coefficient; n is the number of measurement points; T_i is the temperature of the i measurement point, $^{\circ}\text{C}$; \bar{T} is the average temperature, $^{\circ}\text{C}$.

2.3 CFD modeling of greenhouses

Parametric modeling was conducted using the Geometry module in ANSYS FLUENT, and the 1:1 scaled 3D models of the greenhouses were constructed according to their actual size and correlativity (Figure 4). All of the vents were fully opened.

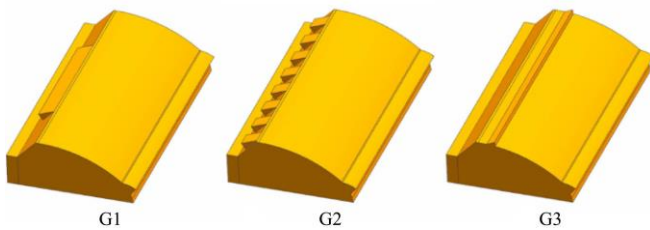


Figure 4 Physical model of investigated greenhouses

The meshing was conducted using ICEM. Specifically, the

polyhedral mesh was chosen, the volume grid was on the order of 400 000, while the number of nodes was on the order of 1.7 million. There was no negative volume when checking the grid quality using the Fluent, indicating that there were no incorrect connections and the following processing could be conducted.

Under the conditions of natural ventilation, the air flow is relative slow, and the temperature alteration during the air motion is negligible, thus the inside air could be regarded as steady incompressible fluid. Consequently, the motion of the air follows the basic physical laws, including:

Mass conservation equation:

$$\text{div}(\rho\bar{u}) = 0 \quad (2)$$

Momentum conservation equation:

$$\begin{cases} \text{div}(\rho\bar{u}\bar{u}) = \text{div}(\mu\text{gard}\bar{u}) - \frac{\partial\bar{p}}{\partial x} + \left[-\frac{\partial(\rho\bar{u}'^2)}{\partial x} - \frac{\partial(\rho\bar{u}'\bar{v}')}{\partial y} - \frac{\partial(\rho\bar{u}'\bar{w}')}{\partial z} \right] \\ \text{div}(\rho\bar{v}\bar{u}) = \text{div}(\mu\text{gard}\bar{v}) - \frac{\partial\bar{p}}{\partial y} + \left[-\frac{\partial(\rho\bar{u}'\bar{v}')}{\partial x} - \frac{\partial(\rho\bar{v}'^2)}{\partial y} - \frac{\partial(\rho\bar{v}'\bar{w}')}{\partial z} \right] \\ \text{div}(\rho\bar{w}\bar{u}) = \text{div}(\mu\text{gard}\bar{w}) - \frac{\partial\bar{p}}{\partial z} + \left[-\frac{\partial(\rho\bar{u}'\bar{w}')}{\partial x} - \frac{\partial(\rho\bar{v}'\bar{w}')}{\partial y} - \frac{\partial(\rho\bar{w}'^2)}{\partial z} \right] \end{cases} \quad (3)$$

Energy conservation equation:

$$\text{div}(\rho\bar{u}\bar{T}) = \text{div}\left(\frac{\lambda}{c_p}\text{gard}\bar{T}\right) + \left[-\frac{\partial(\bar{u}'\bar{T}')}{\partial x} - \frac{\partial(\bar{v}'\bar{T}')}{\partial y} - \frac{\partial(\rho\bar{w}'\bar{T}')}{\partial z} \right] + S_T \quad (4)$$

Composition conservation equation:

$$\text{div}(\rho\bar{u}\bar{c}_s) = \text{div}(D_s\rho\text{gard}\bar{c}_s) + \left[-\frac{\partial(\bar{u}'\bar{c}_s')}{\partial x} - \frac{\partial(\bar{v}'\bar{c}_s')}{\partial y} - \frac{\partial(\bar{w}'\bar{c}_s')}{\partial z} \right] + S_s \quad (5)$$

Assuming the air motion nearby the walls followed the Standard Wall Functions, while the air flow was turbulent flow, the standard k - ε turbulence model was adopted for the simulating calculation as Equation (6):

$$\begin{cases} \text{div}(\rho\bar{u}\bar{k}) = \text{div}\left(\left(\mu + \frac{\mu_t}{\sigma_k}\right)\text{gard}\bar{k}\right) + G_k + \rho\varepsilon \\ \text{div}(\rho\bar{u}\bar{\varepsilon}) = \text{div}\left(\left(\mu + \frac{\mu_t}{\sigma_\varepsilon}\right)\text{gard}\bar{\varepsilon}\right) + \frac{\varepsilon}{k}(C_{1\varepsilon}G_k + C_{2\varepsilon}\rho\varepsilon) \end{cases} \quad (6)$$

where, \bar{u} was the time average of the velocity vector u , m/s; \bar{u} , \bar{v} , \bar{w} were the time average components on the directions x , y , and z , m/s; \bar{u}' , \bar{v}' , \bar{w}' were the pulsating components of u on the directions x , y , and z , m/s; \bar{p} was the time average of the pressure on the fluid microplasm, Pa; \bar{T} was the time average of the temperature T of fluid; T' was the pulsating value of the temperature of the fluid; μ was the viscosity of the fluid, Pa s; ρ was the density of the fluid, kg/m^3 ; λ was the heat conductivity coefficient of the fluid, $\text{W}/(\text{m K})$; c_p was the specific heat capacity of the fluid, $\text{J}/(\text{kg K})$; S_T was the heat source in the fluid; C_s was the time average of the concentration of component s ; C_s' was the pulsating value of the concentration of component s , kg/kg ; D_s was the diffusion coefficient of the component s , m^2/s^2 ; S_s was the production rate of the component s ; k was the turbulence kinetic energy, m^2/s^2 ; ε was turbulent dissipation rate, m^2/s^2 ; μ_t was the turbulent viscosity Pa s; σ_k and σ_ε were the corresponding Prandtl number of the turbulence kinetic energy and the turbulent dissipation rate, which were set as 1.0 and 1.3, respectively in the present study; G_k was the turbulence kinetic energy production

caused by average flow velocity gradient; empirical constants $C_{1\epsilon}$ and $C_{2\epsilon}$ were set as 1.44 and 1.92, respectively.

Solar radiation is one of the key factors affecting the temperature and humidity distribution in the solar greenhouse, thus the irradiative thermal transfer between inside and outside should be taken into consideration. The solar ray tracing method was chosen to load the solar model. According to the studies of Baxevanou et al.^[13], Fidaros et al.^[26] and Zhang et al.^[27], as well as the actual conditions of the tested greenhouse, the Discrete Ordinates (DO) model was chosen, and the radiance equation was given as following:

$$\nabla(I(\vec{r}, \vec{s}) + (a + \sigma_s)I(\vec{r}, \vec{s})) = an^2 \frac{\sigma T^4}{\pi} + \frac{\sigma_s}{4\pi} \int_0^{4\pi} I(\vec{r}, \vec{s}') F(\vec{s}, \vec{s}') ds' \quad (7)$$

where, I was the radiation intensity depending on the position vector \vec{r} and the direction vector \vec{s} ; \vec{s}' was the scattering direction; a , n , and σ_s were the absorption coefficient, refraction coefficient and scattering coefficient, respectively; σ was the Stephen Boltzmann's constant; T was the local temperature; F was the phase function.

As the large Reynolds number of the air motion in greenhouses, the standard $k-\epsilon$ model was chosen and the solar radiation was calculated using DO model. The air inlet on the windward side was set as Velocity Inlet boundary conditions, while the air outlets

on the leeward or on the roof were set as Pressure Outlet boundary conditions. All the windows were opened by rack over hanging style, while the ground and maintenance structures were all set as Wall boundary conditions. The air was regarded as ideal incompressible gas. Specific physical characteristics of the materials used in greenhouse were listed in Table 1.

Table 1 Physical characteristics of the materials used in greenhouse

Materials	Density /kg m ⁻³	Thermal conductivity /W m ⁻¹ ·°C ⁻¹	Specific heat /J kg ⁻¹ ·°C ⁻¹
Air	1.225	0.0242	1006.43
Soil	1400	1.518	840
Wall	1400	0.58	1050
Polysty board	350	0.03	1.38
Pofilm	900	0.29	2550

The boundary conditions used for numerical simulation were the temperature values measured on 16:00 in May 12th, 2019, and the measured data from inside and outside of the greenhouses were used as the initial conditions for the settings of boundary conditions. The polystyrene board was regarded as adiabatic, while the PO film was translucent. The specific parameters of the boundary conditions were listed in Table 2.

Table 2 Specific parameters of the boundary conditions

Name	Materials	Boundary types	Thickness/m	Speed /m s ⁻¹	External radiation intensity /W m ⁻²	External temperature /°C	Transparency
Soil	Soil	Wall	2	-	-	27.3	Opacity
Brickwall	Brick	Wall	0.78	-	-	23.0	Opacity
Polyboard	Polysty	Wall	0.1	-	-	-	Opacity
PO	PO film	Wall	0.0001	-	561.9	29.2	Translucent
Window 1	-	Pressure Outlet	-	-	-	31.4	-
Window 2	-	Velocity Inlet	-	1.51	-	27.6	-

3 Results and discussions

3.1 Model verification

Comparative analysis between the results from experimental test and simulation is the most conventional approach to judge the reliability of simulation results. The comparisons between the measured and simulated temperatures at the same position in G1, G2 and G3 were exhibited by Figure 5, which indicated that there was similar variation tendency in the measured and simulated inside temperature. The mean absolute errors of the 27 measured points from G1, G2 and G3 were 0.8, 0.8 and 0.5 °C, respectively,

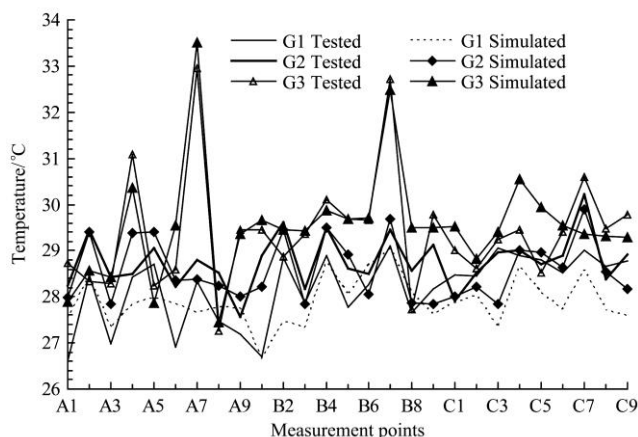


Figure 5 Measured and simulated temperatures in each greenhouse

while the average relative errors were 2.71%, 2.85% and 0.16%, respectively. All the errors between the simulated and measured results were smaller than 5%, indicating that the model could be used in the present study.

3.2 Temperature distribution in the investigated greenhouses

Figure 6 exhibited the distribution of temperature and air flow speed in G1, G2 and G3. The average indoor air temperature in G1, G2 and G3 were 28.0, 28.5 and 29.6 °C, while the temperature uniformity coefficients were 0.44, 0.36 and 1.46, respectively. The outside air sank immediately after entering the greenhouse G1 by the bottom vent on front roof, and then flowed to north to the back wall (Figure 6a). Simultaneously, it brought the upper air to flow to the back window. The wind speed was high in bottom and relatively low in the top. For cross section A and C, the air nearby the back wall climbed to the back roof along the back wall, and subsequently sank along the front roof to form a large eddy. While for cross section B, the air would escape from the vent. As there were vents on the back roof, the air flow in G2 was similar to that in G1. However, as all vents were smaller than that in G1, approximately 1/3 air could not escape but sank along the front roof. The hindered venting led to poor convection heat transfer efficiency. In addition, in the cross section B of G2, obvious turbulent flow was observed in the upper space and the upper of bottom vent (Figure 6c), this also hindered the air cycling. Hence, the temperature in G2 was significantly higher than that in G1 (Figures 6b and 6d). Figures 6b, 6d and 6f indicated that the temperature in G3 was significantly higher than those in G1 and G2,

that might be attributed to the significant shorter air track in G3 (Figure 6e), which causing limited air flow disturbances and air venting, especially the heat accumulation in the top space of the front roof (Figure 6f). It should be noted that, the entrance opened on the gable wall resulted in heat exchange between the indoor and outdoor, and thus lead to the difference of distribution of

temperature close the two gable wall. In this work, the entrance was opened on the gable wall close to section C for greenhouse G3, while it was opened the gable wall close to section A for greenhouse G1 and G2. Therefore, there are differences in distribution of temperature on section A and C, though the positions of them were symmetrical.

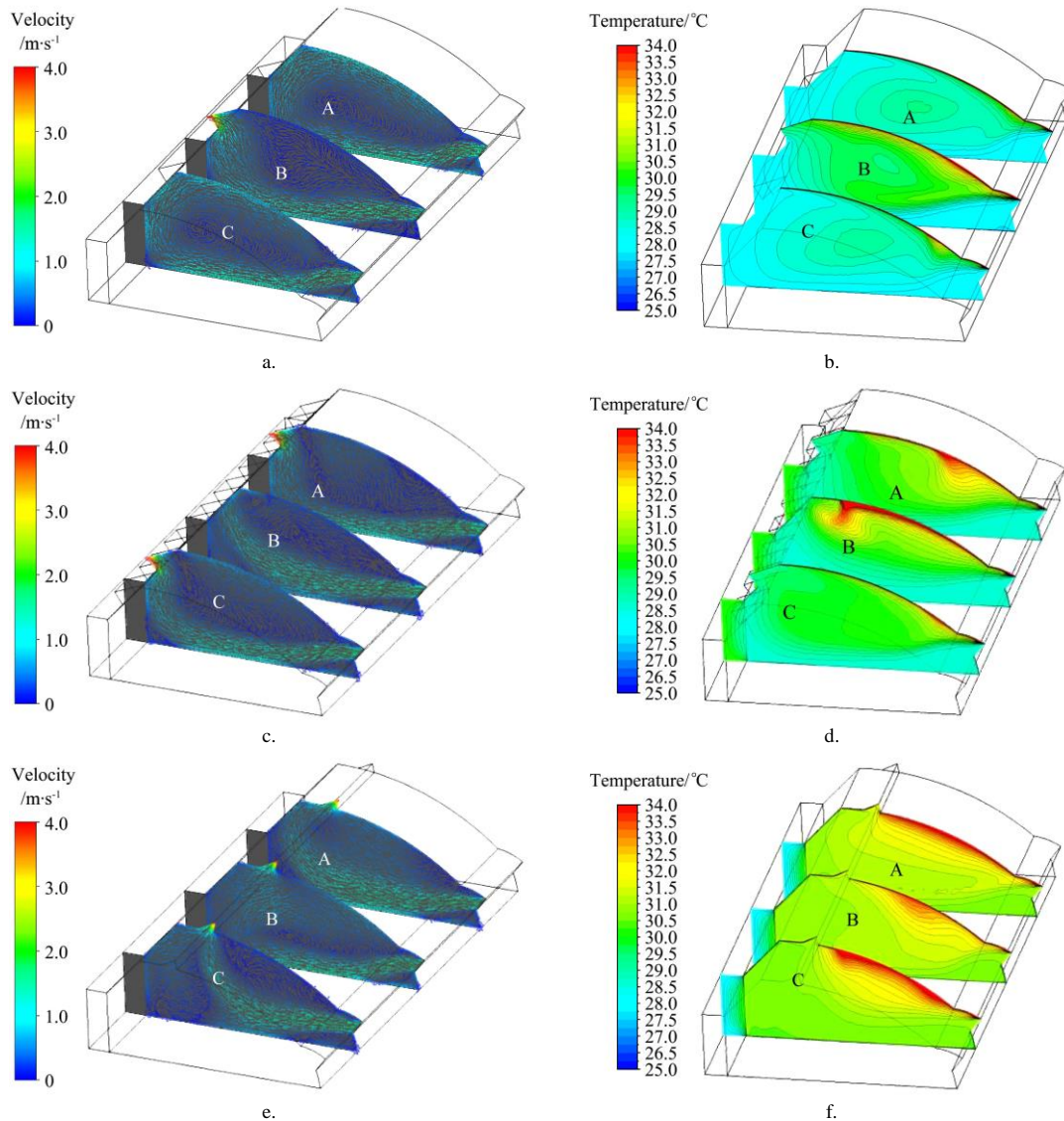


Figure 6 Distribution of air flow field (a, c and e) and temperature field (b, d and f) in greenhouses G1, G2 and G3

3.3 Effects of different combination window opening styles

In order to further explore the heat exchange capacity of greenhouses with different window opening style combinations, following simulation was conducted using the verified CFD model. Same roof vent in G3 was established on the top roof of G1 and G2, and all of the vents were fully opened as well. These 2 new opening styles were recorded as G1+G3 and G2+G3. The simulated results of indoor air flow filed and temperature filed of them were shown in Figure 7, which indicated that the style of G2+G3 significantly alleviated the heat accumulation, and significantly increased the effective disturbance to the inside air flow, especially in the projection area of the back roof. It simultaneously reduced the formation of air cavity, while increased the continuity of the air motion. According to the calculation results, the temperature uniformity coefficients of the style G1+G3 and G2+G3 were respectively 0.52 and 0.36, which revealed that the combination of spaced back roof ventilation and

top roof ventilation exhibited the best cooling effects and temperature uniformity. The average temperature on the cross sections A, B and C in each ventilation style also confirmed this result (Figure 8).

The effects of outside environment and window opening on the temperature distribution and air flow velocity in multi-span greenhouse and plastic tunnel had been extensively investigated^[26,28]. CFD was also used for the analysis of the temperature and humidity environments and the airflow field in solar greenhouse^[29-31]. However, studies on the temperature distribution and air motion regularity in the solar greenhouse with different window opening style are lacking. In the present study, simulation modeling of the solar greenhouse without crop plantation was conducted based on the existing studies on the inside microenvironment distribution in plant-free greenhouse using CFD^[32,33], and the influence of window opening style on the indoor environment was investigated. It was noteworthy that in

the present study, only the thermal interaction among the floor, front roof, back roof, back wall and outside were considered, while the effects of the plants on the inside thermal environment, such as their transpiration and the heat convection between leaves and air, were not concerned. Hence, in the solar greenhouse planting crops with large leaf area index, the simulated models in this study should be further modified. In addition, the verification of the natural ventilation model simulated results was only conducted basing on the data of the temperature detecting points, but not on those of the air velocity detecting points. Thus, the results could only provide theoretical analysis of the distribution of air flow

velocity. Considering the effects of crops were not considered, the simulated temperature would be higher than the detected values, and the air flow simulation would be affected either. In the following investigation, the porous model and transpiration model would be introduced into the simulation to optimize the parameters in the model and thus increase its simulation accuracy. On the other hand, as the crops would hinder the air motion in natural ventilation conditions, thus the tall crops, such as pepper, tomato and cucumber, should be regarded as solid media with given porosity, and their air flow resistance should be also considered for increasing the simulation accuracy of models.

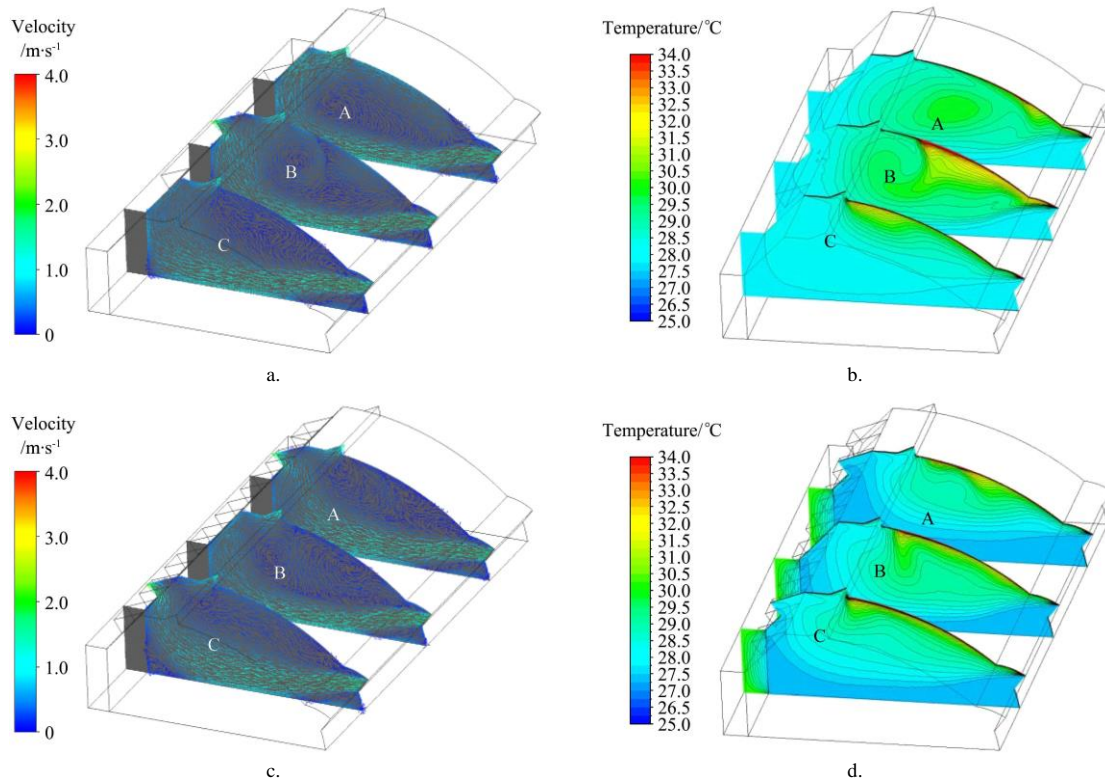


Figure 7 Distribution of air flow and temperature field in the greenhouse with different window opening style combinations

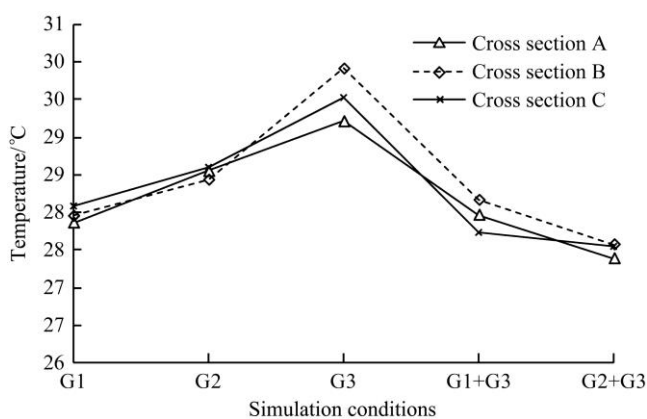


Figure 8 Average temperature of cross section A (red), B (purple) and C (yellow) under different window opening styles s

4 Conclusions

(1) The CFD model of different window opening styles was built according to the standard $k-\epsilon$ turbulence model and DO radiation model. The simulated and measured temperatures at different points located at three typical sections of the greenhouses exhibited favorable agreement, indicating the built model is suitable to simulation.

(2) In the case of the windows opening area is the same and only single ventilation style is applied, back roof full opening style exhibited the best cooling effect. The inside average temperature of the greenhouse with G1 style decreased respectively 0.5 and 1.6 °C than that of the greenhouse with G2 and G3.

(3) The cooling effect of the window opening style of G2+G3 was more favorable than that of the style of G1+G3. The style of G2+G3 exhibited better cooling effect than the single ventilation styles, with the lowest temperature (27.5 °C) and temperature uniformity coefficient (0.36).

Acknowledgements

This research was financially supported by National Natural Science Foundation of China (31901420) and Shaanxi Provincial Key Research and Development Program (2019TSLNY01-03).

[References]

- [1] Li T L. Current situation and prospects of green house industry development in China. *Journal of Shenyang Agricultural University*, 2005; 36(2): 131–138. (in Chinese)
- [2] McCartney L, Lefsrud M G. Field trials of the natural ventilation augmented cooling (NVAC) greenhouse. *Biosystem Engineering*, 2018; 174: 159–172.
- [3] Villagrán E A, Romero E J B, Bojacá C R. Transient CFD analysis of the

- natural ventilation of three types of greenhouses used for agricultural production in a tropical mountain climate. *Biosystem Engineering*, 2019; 188: 288–304.
- [4] Yang Z C, Optimal wind speed and CFD simulation in sunlight greenhouse. Doctor dissertation. Yangling: Northwest A&F University, 2006. (in Chinese)
- [5] Mistriotis A, Bot G, Picuno P, Scarascia-Mugnozza G. Analysis of the efficiency of greenhouse ventilation using computational fluid dynamics. *Agricultural and Forest Meteorology*, 1997; 85(3-4): 217–228.
- [6] Wei B, Guo S R, Wang J, Li J, Wang J W, Zhang J, et al Thermal performance of single span greenhouses with removable back walls. *Biosystems Engineering*, 2016; 141: 48–57.
- [7] Xie D, Xu H, Li T L, Wang R. Effects of top natural ventilation on temperature and humidity in greenhouse. *Jiangsu Agricultural Sciences*, 2010; 6: 573–575. (in Chinese)
- [8] Yadav A S, Bhagoria J L. Heat transfer and fluid flow analysis of solar air heater: A review of CFD approach. *Renewable and Sustainable Energy Reviews*, 2013; 23: 60–79.
- [9] Norton T, Sun D-W, Grant J, Fallon R, Dodd V. Applications of computational fluid dynamics (CFD) in the modelling and design of ventilation systems in the agricultural industry: A review. *Bioresource Technology*, 2007; 98(12): 2386–2414.
- [10] Zhai Z Q, Chen Q Y. Numerical determination and treatment of convective heat transfer coefficient in the coupled building energy and CFD simulation. *Building and Environment*, 2004; 39(8): 1001–1009.
- [11] Bhutta M M A, Hayat N, Bashir M H, Khan A R, Ahmad K N, Khan S. CFD applications in various heat exchangers design: A review. *Applied Thermal Engineering*, 2011; 32: 1–12.
- [12] Bournet P-E, Boulard T. Effect of ventilator configuration on the distributed climate of greenhouses: A review of experimental and CFD studies. *Computers and Electronics in Agriculture*, 2010; 74(2): 195–217.
- [13] Baxevanou C, Fidaros D, Bartzanas T, Kittas C. Numerical simulation of solar radiation, air flow and temperature distribution in a naturally ventilated tunnel greenhouse. *Agricultural Engineering International CIGR Journal*, 2010; 12(3): 48–67.
- [14] Song D. Research on soil wall of solar greenhouse and simulation of its temperature environment. Master dissertation. Yangling: Northwest A&F University, 2013. (in Chinese)
- [15] Chang L N. Experimental and simulation research of the thermal and moisture environment in a passive greenhouse. Master dissertation. Jinan: Shandong Jianzhu University, 2011. (in Chinese)
- [16] Fang H, Yang Q T, Zhang Y, Lu W, Zhou B, Zhou S. Simulation performance of a ventilated greenhouse based on CFD technology. *Chinese Journal of Agrometeorology*, 2015; 36(2): 155–160.
- [17] Fang H, Yang Q C, Zhang Y, Lu W, Zhou B, Zhou S. Simulation performance of a ventilated greenhouse based on CFD technology. *Chinese Journal of Agrometeorology*, 2015; 36(2): 155–160. (in Chinese)
- [18] Zhang F, Fang H, Yang Q C, Cheng R F, Zhang Y, Ke X L, et al. Ventilation simulation in a large-scale greenhouse based on CFD. *Chinese Journal of Agrometeorology*, 2017; 38(4): 221–229. (in Chinese)
- [19] Zhang X, Wang H L, Zou Z R, Wang S J. CFD and weighted entropy based simulation and optimisation of Chinese Solar Greenhouse temperature distribution. *Biosystems Engineering*, 2016; 142: 12–26.
- [20] Tong G, Christopher D M. Temperature variations with various enclosure material thermal property for a Chinese solar greenhouse. ASABE annual international meeting, Spokane, Washington, July 16-19, 2017.
- [21] Gupta P K, Pappuru S, Gupta S, Patra B, Chakraborty D, Verma R S. Self-assembled dual-drug loaded core-shell nanoparticles based on metal-free fully alternating polyester for cancer theranostics. *Materials Science & Engineering C: Materials for Biological Applications*, 2019; 101: 448–463.
- [22] He K S, Chen D Y, Sun L J, Liu Z L. Effects of vent configuration and span number on greenhouse microclimate under summer conditions in Eastern China. *International Journal of Ventilation*, 2016; 13(4): 381–396. (in Chinese)
- [23] Zhou C J. A solar greenhouse with light-transparent rear roof covered by active heat preservation quilt. *Agricultural Engineering Technology*, 2015; 35(16): 24–26. (in Chinese)
- [24] Zhou C J. The crystallization of greenhouse technology between China and Israel—Eisenberg's improvement and innovation of China's Solar Greenhouse. *Agricultural Engineering Technology*, 2017; 37(16): 44–50. (in Chinese)
- [25] Cheng X H, Mao H P, Wu D L. Research progress on natural ventilation in greenhouse. *Journal of Anhui Agriculture Science*, 2009; 37(8): 3803–3805. (in Chinese)
- [26] Fidaros D K, Baxevanou C A, Bartzanas T, Kittas C. Numerical simulation of thermal behavior of a ventilated arc greenhouse during a solar day. *Renewable Energy*, 2009; 35(7): 1380–1386.
- [27] Zhang G X, Fu Z T, Yang M S, Liu X X, Dong Y H, Li X X. Nonlinear simulation for coupling modeling of air humidity and vent opening in Chinese solar greenhouse based on CFD. *Computers and Electronics in Agriculture*, 2019; 162: 337–347.
- [28] Khaoua S O, Bournet P, Migeon C, Boulard T, Chassériaux G. Analysis of greenhouse ventilation efficiency based on computational fluid dynamics. *Biosystems Engineering*, 2006; 95(1): 83–98.
- [29] Reddy H M, Vinod A V. CFD simulation of the heat transfer using nanofluids in microchannel with dimple and protrusion. *Indian Chemical Engineer*, 2019; 61(1): 1–12.
- [30] Chen J L, Cai Y W, Xu F, Hu H G, Ai Q L. Analysis and optimization of the fan-pad evaporative cooling system for greenhouse based on CFD. *Advances in Mechanical Engineering*, 2014; 2014(3): 1–8.
- [31] Molina-Aiz F D, Valera D L, López A. Airflow at the openings of a naturally ventilated Almería-type greenhouse with insect-proof screens. *International Symposium on High Technology for Greenhouse Systems Greensys*, 2011; 893: 545–552.
- [32] Li Y, Wu D, Yu Z. Simulation and test research of micrometeorology environment in a sun-light greenhouse. *Transactions of the Chinese Society of Agricultural Engineering*, 1994; 10(1): 130–136.
- [33] Kim K, Yoon J-Y, Kwon H-J, Han J-H, Son J E, Nam S-W, et al. 3-D CFD analysis of relative humidity distribution in greenhouse with a fog cooling system and refrigerative dehumidifiers. *Biosystems Engineering*, 2008; 100(2): 245–255.